

Characterizing RNA Nanoparticles by Analytical Ultracentrifugation

Abstract

Chad T. Schwartz^{1*}, Daniel Jasinski^{2*}, and Peixuan Guo^{2*}

¹Beckman Coulter, Inc., Indianapolis, IN 46268

²University of Kentucky, Department of Pharmaceutical Sciences, Lexington, KY 40506

*Authors contributed equally

RNA nanotechnology is gaining in popularity due to its simplistic and rational design for creating nanostructures for applications in medicine and therapeutics. RNA nanosquares were previously designed and constructed demonstrating the tunable size and stability of RNA as a nanoparticle delivery system¹. Dynamic light scattering (DLS) and atomic force microscopy (AFM) were utilized to characterize the size and shape of the squares verifying the molecular model and native PAGE assembly data. Here, we display the use of analytical ultracentrifugation (AUC) to further validate the size of the nanostructures, promoting the use of the instrument as an orthogonal tool for nanoparticle characterization and provide insights into applications where AUC provides distinct advantages for nanoparticle characterization over other sizing methods.

Introduction

Recent achievements in RNA nanotechnology have led to its growth as a platform for nanomedicine and therapeutics. RNA has many unique advantages which situate it favorably as a delivery device including its defined size, structure, stoichiometry, modular design, and ability to be produced in large quantities in a cell-free system. RNA can be manipulated with the simplicity of DNA but displays the versatility in structure and function similar to proteins. Previous work by Guo et. al. has detailed the structure and function of RNA nanoparticles derived from phi29 bacteriophage packaging RNA (pRNA)¹⁻¹³. These pRNA-based structures have previously been characterized and functionalized for therapeutics and have even demonstrated efficacy as a delivery system for therapeutics¹⁴⁻¹⁸.

Size and shape of nanoparticles are important factors for delivery, efficacy, biodistribution, and circulation time¹⁶. Jasinski et. al. demonstrated the ability to control the size

and shape of RNA nanosquares and the feasibility to fine-tune the physicochemical properties of these particles¹. Several techniques are currently available for measuring size and shape of particles such as dynamic light scattering and size exclusion chromatography but analytical ultracentrifugation offers many significant advantages over these methods. In our studied system presented here, Jasinski et. al. designed and then annealed RNA strands to form square-like structures¹. Particle assembly was initially analyzed by native polyacrylamide gel electrophoresis (PAGE) and the expected size matched well with the molecular weight marker. The three designed RNA squares were then characterized by both AFM and DLS. In the analysis, AFM images were obtained that validated the proper assembly and, with fair resolution, determined the diameter of each square. Dynamic light scattering was then used to characterize particle size, measuring hydrodynamic diameters of 4.0 ± 0.9 nm, 11.2 ± 1.3 nm, and 24.9 ± 1.5 nm for the expected 5, 10, and 20 nm squares, respectively¹.

Materials & methods

- **RNA Oligo Construction:** Detailed methods for nanoparticle design and construction have been previously discussed in detail^{4,17}. Briefly, two “arms” of the pRNA-3WJ were extended by 8 base pair helices using Swiss PDB Viewer followed by alignment of four 3WJ modules in a planar configuration, resulting in square geometry. Construction of different size nanosquares was achieved by addition or removal of base pairs connecting each 3WJ module.
- **RNA Purification:** RNA strands were prepared either by in vitro transcription of synthetic DNA coding for the antisense sequence of square strands containing the T7 promoter or by solid phase

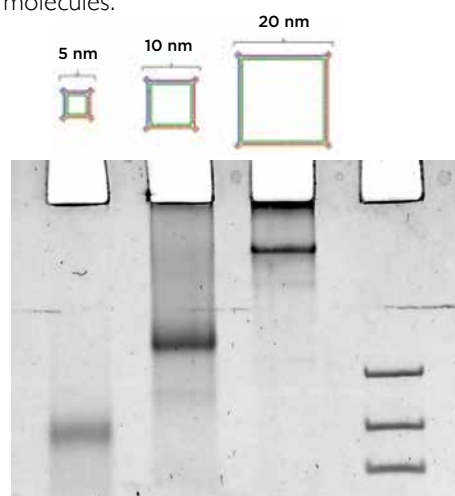
synthesis using a standard phosphoramidite chemistry method. Modified RNA strands (2'-deoxy-2'fluoro) were prepared by in vitro transcription with the Y639F mutant T7 polymerase and 2'F modified dCTP and dUTP. Transcribed RNA oligomers were purified by 8 M urea polyacrylamide gel electrophoresis (PAGE) and standard desalting procedures were used for chemically synthesized oligomers. Cy5 labeling was performed using standard phosphoramidite chemistry and dye-labeled oligomers were purified by ion-pair reverse phase (IPRP) HPLC.

- **Nanosquare HPLC Purification:** IPRP chromatography was used to purify pre-assembled nanosquares with acetonitrile and water in .1 M triethylammonium acetate (TEAA) used as the mobile phase. A linear gradient of 5% to 30% acetonitrile was run over 30 minutes at a flow rate of 1.5 mL/min. The retention time of the 10 nm nanosquare was assayed by overlapping absorbance at 260 nm (RNA) and 650 nm (fluorophore). Fractions were collected and vacuum dried on low heat. Dried samples were then re-suspended in 1X TMS buffer and combined.
- **Assembly of RNA Nanoparticles:** Equimolar amounts of RNA oligomers were mixed to a final concentration of 20 μ M in TMS buffer (40 mM Tris-HCl, 10 mM MgCl₂, 100 mM NaCl). The mixture was heated to 80°C for 5 min and then slowly cooled to 4°C at a rate of 2°C/min on an Eppendorf Mastercycle thermocycler. Confirmation of the assembly products were then run on native PAGE.
- **Native PAGE:** All assembly experiments were performed on 7% (29:1) native PAGE and run at 100 V in a 4°C cold room for 120 min. Cy5-labeled RNAs were then scanned on a Typhoon FLA 7000, and total RNAs were stained with ethidium bromide (EB).
- **AUC of RNA Nanoparticles:** Sedimentation velocity experiments were performed in a Beckman Coulter Proteome Lab XL-I (Beckman Coulter) following standard protocols, set to scan with both interference and absorbance optics, measuring at a wavelength of 260 nm, for 4 hours, at 20°C. Samples of RNA squares were loaded ($A_{260} \sim 0.5$) into 2-channel 12 mm path length sector shaped cells and thermally equilibrated at zero speed. Absorbance and interference velocity scans were subsequently acquired at 50,000 rpm. Absorbance data were analyzed in SEDFIT 14.7g (www.analyticalultracentrifugation.com) and DCDT+ (<http://www.jphilo.mailway.com/dcdt+.htm>). In all cases excellent fits were observed with low root mean square deviations. The partial specific volume of RNA nanoparticles was fixed at 0.55. The density ρ and viscosity η for TMS were calculated in SEDNTERP (<http://sednterp.unh.edu>).
- **Dynamic Light Scattering:** The translational diffusion coefficients D and hydrodynamic diameters D_h were

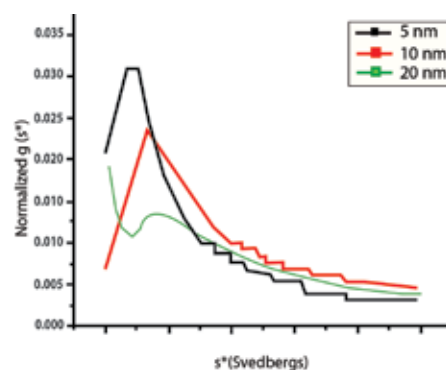
determined from an autocorrelation analysis of the scattered light at 514.5 nm on a Beckman Coulter DelsaMax Pro. Twenty DLS acquisitions of 5 seconds each were ran with no auto-attenuation with peak radius cut-offs between 0.5 nm and 30 nm. Data was exported from the DelsaMax software package and put into Origin for plotting.

Results

Following particle assembly, all three RNA squares were analyzed by Native PAGE for assembly. The squares migrated correctly based on molecular weight of the full assembly (Fig. 1A) suggesting that annealing was efficient. A low percentage of single strand oligomers were visible in the acrylamide gel despite no extensive purification. The three differently sized RNA squares were then analyzed for sedimentation coefficient using sedimentation velocity analytical ultracentrifugation. Data was exported and analyzed for sedimentation coefficient. The 5 nm, 10 nm, and 20 nm RNA squares were determined to have peak sedimentation coefficients of 4.25 S, 7.25 S, and 8.8 S, respectively (Fig. 1B). As expected, the larger molecules had higher sedimentation coefficients than the smaller molecules. peak sedimentation coefficients of 4.25 S, 7.25 S, and 8.8 S, respectively (Fig. 1B). As expected, the larger molecules had higher sedimentation coefficients than the smaller molecules.



(A)



(B)

Figure 1A A) Native polyacrylamide gel electrophoresis (PAGE) of three different sized RNA nanoparticles. B) Least-squared regression fit of sedimentation velocity experiment of 5 nm, 10 nm, 20 nm nanoparticles.

To determine whether or not diluting the samples affected the sedimentation coefficient, the 10 nm square was diluted 3-fold. The non-diluted and the diluted samples were again analyzed and the sedimentation coefficient was determined to be 6.6 S and 6.75 S, respectively, suggesting that after dilution, the particle remains assembled and sediments as the monomeric unit (Fig. 2).

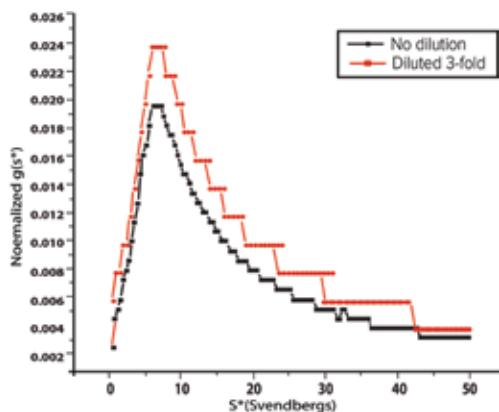


Figure 2. Least-squared regression fit of sedimentation velocity experiment of a diluted and non-diluted 10 nm RNA square.

In efforts to scale up production, better track the nanoparticles, and increase stability, Cy5 was conjugated to the 10 nm particle and the bases were modified and annealed using 2'F bases and then purified by reverse phase high performance liquid chromatography (HPLC). Replacing the 2' hydroxyl group with a 2' fluorine group reduces the particles' susceptibility to RNase degradation. HPLC was effective at separating the free unlabeled dye from the conjugated particle (Fig. 3A) at a retention time of 25-29 minutes. Furthermore, the HPLC trace suggested that the modified particle was present in two separate conformations or sizes as a minor shoulder peak is evident to the right of the major peak. This shoulder was present in both the 260 nm and 650 nm absorbance, suggesting that the species contained both nucleic acid and dye, respectively.

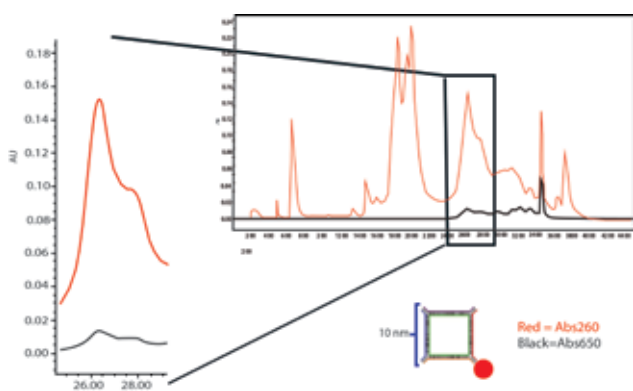


Figure 3. HPLC chromatogram of 2'F-modified 5'Dy647 10 nm RNA square. The red trace represents Abs260 and the black trace represent Abs650 for nucleic acid absorption and dye absorption, respectively.

Although the HPLC was powerful in providing separation and species identification, it did not provide the intricate details of species size or sedimentation coefficient. Dynamic

light scattering is an essential and common tool used in many particle characterization labs. This method measures particles in solution and, based on the amount of scattered light detected, calculates a hydrodynamic radius of the particle of interest. Here, we utilized Beckman Coulter's DelsaMax Pro to analyze the size of the purified 2'F-5'Cy5 10 nm RNA square. A series of acquisitions were summarized and plotted for hydrodynamic diameter (Fig. 3B). The resulting plot generated a large peak centered on 10 nm but tailed towards the right, perhaps indicative of a larger species.

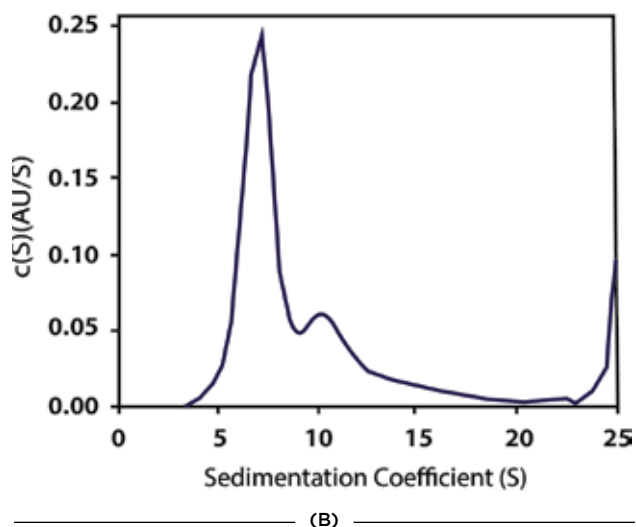
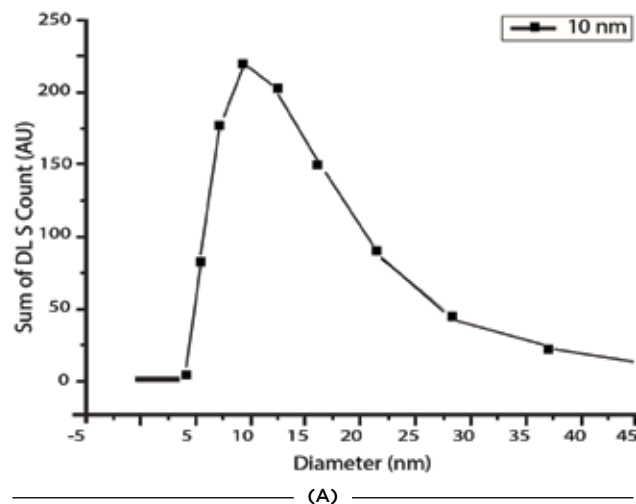


Figure 4. A) Dynamic light scattering plot of HPLC-purified 10 nm RNA square. B) Sedimentation velocity $c(s)$ analysis of HPLC-purified 10 nm RNA square.

Finally, the 2'F-5'Cy5 10 nm RNA square was subjected to analytical ultracentrifugation to determine the presence of heterogeneity and relative amount of the larger species. Upon $c(s)$ analysis using the popular software SEDFIT, the major species at a weight signal average of over 57% was identified at 7.09 S, a value that corresponds nicely to the previous analysis of the unmodified square. Additionally a minor (13.3% signal weight average) 10.21 S peak was identified (Fig. 3C). It is essential to note that the AUC was able to resolve the two species where the DLS method failed. Analysis of analytical ultracentrifugation data often involves characterizing the stoichiometry or oligomeric

state of particles. If we assume that the oligomeric shape is similar to that of the monomeric shape, then its stoichiometry, N , can be described as $(S_N/S_1)^{1.5}$, where S_N is the sedimentation coefficient of the N -mer and S_1 is the sedimentation coefficient of the monomer. For a sphere, as a rule of thumb, a value of 1.45 indicates a dimer. Here, we obtain a value of 1.44 (10.21/7.09), a value highly indicative of a dimeric species. It is highly conceivable that the particles assembled together during annealing and the result was a dimeric assembly, larger in size than the 20 nm RNA square due to its unorthodox shape.

Discussion

Analytical ultracentrifugation is a powerful biophysical technique with a storied history dating back to the early part of the twentieth century. The technique was primarily used to demonstrate the existence of macromolecules following the ground-breaking research performed by Theodor Svedberg and colleagues where it was determined that hemoglobin was a monodisperse species around 68 kDa. He was subsequently awarded the Nobel Prize for his work on colloids and disperse systems using an early version of the technology.

AUC offers significant advantages over orthogonal techniques for nanoparticle characterization. In nanoparticle design, it is often necessary to assess polydispersity. Impurities, conformational changes, and conjugation efficiency are all critical to nanoparticle efficacy and biodistribution. Heterogeneity is typically not quantified in orthogonal techniques such as AFM and DLS. However, in AUC, the distribution of sedimenting species is quantifiable and reported with high precision.

Since the goal of many nanoparticles is to be distributed throughout the body as a therapeutic, it is critical that analysis is performed prior to lengthy and expensive clinical trials. AUC is executed in a buffer of choice, analyzed free in solution, and not conjugated or adsorbed to a surface, or ionized, melted, or magnetized for investigation. This allows researchers to measure environmental effects such as pH, temperature, salt concentration, and much more in a single run.

Here, we validated the previous results from orthogonal technologies such as DLS and AFM as reported in Jasinski, et. al. Furthermore, concentration effects were assayed and it was determined that the molecule is stable and forms homogenous particles at low concentration. Lastly, after modification for stability and identification, followed by purification, the RNA particles were again analyzed by light scattering and AUC and the particle of interest retained the expected size and conformation of the monomeric unit but also most likely assembled into a dimer as well. This information is critical as it informs researchers that the particle of interest has changed size and shape and this change is quantifiable in terms of percent species and size.

Acknowledgements

The authors would like to thank Dr. Peixuan Guo, Endowed Chair in Nanobiotechnology, at the University of Kentucky, College of Pharmacy for kindly providing material and direction.

Disclaimer

All trademarks are the property of their respective owners. Beckman Coulter, the stylized logo, and ProteomeLab XL-I are all trademarks of Beckman Coulter, Inc. and are registered with the USPTO. For Beckman Coulter's worldwide office locations and phone numbers, please visit www.beckmancoulter.com/contact

References

1. Jasinski DL, Khisamutdinov EF, Lyubchenko YL, Guo P. Physicochemically Tunable Polyfunctionalized RNA Square Architecture with Fluorogenic and Ribozymatic Properties. *ACS Nano*. 2014 Jul 21.
2. Guo P. 2010. The emerging field of RNA nanotechnology. *Nature Nanotechnology*. 5, 833
3. Shu D, Zhang H, Petrenko R, Meller J, and Guo P. 2010. Dual-Channel Single-Molecule Fluorescence Resonance Energy Transfer to Establish Distance Parameters for RNA Nanoparticles. *ACS Nano*, 4 (11), 6843–6853
4. Liu J, Guo S, Cinier M, Shlyakhtenko L, Shu Y, Chen C, Shen G, and Guo P. 2011. Fabrication of Stable and RNase- Resistant RNA Nanoparticles Active in Gearing the Nanomotors for Viral DNA Packaging. *ACS Nano*. 5 (1), 237
5. Guo P. 2011. RNA Nanotechnology: methods for synthesis, conjugation, assembly and application of RNA nanoparticles. *Methods*. 54(2):201-3.
6. Shu Y, Cinier M, Fox SR, Ben-Johnathan N, Guo P. 2011. Assembly of Therapeutic pRNA-siRNA Nanoparticles Using Bipartite Approach. *Mol Ther*. 19(7):1304-11.
7. Guo P, Haque F, Hallahan B, Reif R, Li H. Uniqueness, advantages, challenges, solutions, and perspectives in therapeutics applying RNA nanotechnology. *Nucleic Acid Ther*. 2012 Aug;22(4):226-45.
8. Shu Y, Haque F, Shu D, Li W, Zhu Z, Kotb M, Lyubchenko Y, Guo P. Fabrication of 14 different RNA nanoparticles for specific tumor targeting without accumulation in normal organs. *RNA*. 2013 Jun;19(6):767-77. doi: 10.1261/rna.037002.112. Epub 2013 Apr 19.
9. Zhang H, Endrizzi J, Shu Y, Haque F, Sauter C, Shlyakhtenko L, Lyubchenko Y, Guo P, Chi Y. Crystal Structure of 3WJ Core Revealing Divalent Ion-promoted Thermostability and Assembly of the Phi29 Hexameric Motor pRNA. *RNA* 2013 Sep;19(9):1226-
10. Haque F, Guo P. Overview of methods in RNA nanotechnology: synthesis, purification, and characterization of RNA nanoparticles. *Methods in Molecular Biology*. 2015;1297:1-19.
11. Jasinski DL, Schwartz CT, Haque F, Guo P. Large scale purification of RNA nanoparticles by

- preparative ultracentrifugation. *Methods in Molecular Biology*. 2015;1297:67-82.
12. Khisamutdinov EF, Jasinski DL, Guo P. RNA as a Boiling-Resistant Anionic Polymer Material To Build Robust Structures with Defined Shape and Stoichiometry. *ACS Nano*. 2014 May 27;8(5):4771-81.
 13. Shu Y, Cinier M, Shu D and Guo P. 2011. Assembly of Multifunctional Phi29 pRNA Nanoparticles for Specific Delivery of siRNA and other Therapeutics to Targeted Cells. *Methods*. 54(2):204-14.
 14. Shu D, Shu Y, Haque F, Abdelmawla S and Guo P. 2011. Thermodynamically stable RNA three-way junction for constructing multifunctional nanoparticles for delivery of therapeutics. *Nature Nanotechnology*. 6(10):658-67.
 15. Haque F, Shu D, Shu Y, Shlyakhtenko L, Rychahou P, Evers M, Guo P. Ultrastable synergistic tetravalent RNA nanoparticles for targeting to cancers. *Nano Today*. 2012 Aug;7(4):245-57.
 16. Shu Y, Shu D, Haque F, Guo P. Fabrication of pRNA Nanoparticles to Deliver Therapeutic RNAs and Bioactive Compounds into Tumor Cells. *Nature Protocols*. 8, 1635-1659 (2013).
 17. Shu D, Khisamutdinov E, Zhang L and Guo P. Programmable folding of fusion RNA in vivo and in vitro driven by pRNA 3WJ motif of phi29 DNA packaging motor. *Nucleic Acids Res*. 2014 Jan;42(2):e10.
 18. Shu Y, Pi F, Sharma A, Rajabi M, Haque F, Shu D, Leggas M, Evers BM, Guo P. Stable RNA nanoparticles as potential new generation drugs for cancer therapy. *Adv Drug Deliv Rev*. 2014 Feb;66C:74-89.